Stochastic Modeling of Passive Scalar Transport in Turbulent Channel Flows at High Schmidt Numbers

Marten Klein

Department of Numerical Fluid and Gas Dynamics
Brandenburg University of Technology
Siemens-Halske-Ring 14, D-03046 Cottbus, Germany
marten.klein@b-tu.de

Heiko Schmidt

Department of Numerical Fluid and Gas Dynamics
Brandenburg University of Technology
Siemens-Halske-Ring 14, D-03046 Cottbus, Germany
heiko.schmidt@b-tu.de

ABSTRACT

High-Schmidt number flow simulations are challenging since the flow has to be resolved down to the Batchelor scale, which yields high resolution requirements. In order to close the gap between the flow regime of applications and that reachable by numerical simulations, we utilize a stochastic modeling approach, the so-called One-Dimensional Turbulence (ODT) model. In the present study, ODT is used as stand-alone tool to investigate the turbulent transport of a passive scalar for Schmidt numbers $1 \leq Sc \leq 5000$ in incompressible, fully-developed turbulent channel flows for Reynolds numbers $Re_\tau \leq 2000$. The applicability of ODT is assessed by comparing the scalar mean and the root mean square fluctuations to those of reference Direct Numerical Simulations (DNS) and Large-Eddy Simulations (LES) up to $Sc = 400$. Good qualitative but also quantitative agreement is observed between DNS, LES, and ODT, but ODT underestimates the mean scalar concentration in the bulk by a factor of $\approx 3/4$. Otherwise, ODT exhibits the correct boundary layer structure and yields the von Kármán constant for the scalar as $\kappa_\theta = 0.23$, which corresponds well to the available reference DNS/LES. ODT is then used to simulate the scalar mass transfer coefficient K^+ up to very high Schmidt numbers. The power law $K^+_{\mathrm{ODT}} \propto Sc^{-0.651}$ is obtained for $Sc > 100$ where it is also independent of the Reynolds number. This corresponds to the reference laboratory measurements and DNS/LES, which obey $K^+_{\mathrm{lab}} \propto Sc^{-0.704}$. The present study shows that ODT can be a versatile tool for robust and accurate modeling of the turbulent scalar transport up to very high Schmidt and Reynolds numbers.

INTRODUCTION

The turbulent transport of a passive scalar (like small temperature variations, a single tracer, dye, or smoke) is relevant for many technical applications, for example, to study the cooling rate of a technical device under different operation conditions. Numerical simulations of related flow problems have remained a challenging task due to the resolution requirements imposed by the development of very small scales in the flow. That is, the scalar field exhibits spatial scales as small as the Batchelor scale $\eta_{\mathrm{B}} = Sc^{-1/2}\eta_{\mathrm{K}}$ (Batchelor, 1959), which can be much smaller than the Kolmogorov scale η_{K} when the Schmidt number $Sc \equiv \nu/\Gamma$ (kinematic viscosity ν, scalar diffusivity Γ) is much larger than unity. It is crucial to resolve the small scale dynamics everywhere in the flow in order to predict the spatio-temporal distribution of the scalar correctly and, hence, the scalar mass transfer rate across the wall. Past (e.g Shaw & Hanratty, 1977) and recent studies (e.g. Na *et al.*, 1999; Schwertfirm & Manhart, 2007; Hasegawa & Kasagi, 2009; Ostilla-Monico *et al.*, 2015) investigated how the turbulent scalar transport depends on the Schmidt and Reynolds number. The conclusion from these studies is that the turbulent scalar transport is not fully analogous to the turbulent momentum transport, so that a "simple parameterization" of the scalar transport is often not permissible.

Recent numerical studies used different methods to study the phenomena governing the scalar transport. The methods encompass multi-resolution strategies (e.g. Schwertfirm & Manhart, 2007; Ostilla-Monico *et al.*, 2015), hybrid resolution approaches (e.g. Hasegawa & Kasagi, 2009), or Langrangian methods (e.g. Na *et al.*, 1999). All of them basically avoid a costly over-resolution of the velocity field by computing only the passive scalar on a finer grid. The Lagrangian methods exploit in addition that the passive scalar has no feedback on the flow evolution due to which the velocity field is prescribed for the scalar evolution. This decoupling of the scalar and momentum evolution cannot be used for buoyant or reacting flows, so that Eulerian methods have also been used for an investigation of the passive scalar transport. These Direct Numerical Simulations (DNS) or high-resolution Large-Eddy Simulations (LES) are currently feasible only for Schmidt numbers $Sc \leq 1000$ provided that the Reynolds number is rather small, say $Re_\tau \leq 200$, where $Re_\tau \equiv u_\tau \delta/\nu$ is the friction Reynolds number (with the friction velocity u_τ and the channel half-height δ). In laboratory experiments and applications, however, both the Schmidt and the Reynolds number may easily exceed 10^4 (as in Shaw & Hanratty, 1977, for example).

In the present study, we utilize the One-Dimensional Turbulence (ODT) model to make turbulent channel flow simulations feasible at high Schmidt and Reynolds numbers. ODT resolves all spatial scales of the flow by stochastically modeling the temporal evolution of property profiles along a notional line of sight through the three-dimensional (3-D) turbulent flow. In this paper, ODT results of turbulent channel flows up to $Sc \sim 10^4$ and $Re_\tau \sim 10^3$ are reported.

The rest of this paper is organized as follows. First, the application of ODT to the simulation of turbulent channel flows with a passive scalar is outlined. Second, mean and fluctuation profiles obtained by ODT are compared to available DNS/LES results for moderately high Schmidt numbers ($1 \leq Sc \leq 400$). Third, the scalar mass transfer coefficient obtained by ODT is compared to available numerical data and laboratory measurements up to very high Schmidt numbers ($Sc \leq 5000$). The paper closes with a summary and concluding remarks.

ODT APPLIED TO TURBULENT CHANNEL FLOWS

The One-Dimensional Turbulence (ODT) is a relatively new approach for multi-scale modeling of turbulent transport (Kerstein, 1999; Kerstein *et al.*, 2001). The adaptive numerical solver used for this work has been described by Lignell *et al.* (2013). In the following, we first outline central aspects of ODT, then move on to the channel flow configuration, and finally discuss typical flow profiles.

ODT in a Nutshell

The central idea of ODT is to model dimensions rather than scales by simulating a turbulent flow only on a notional line of sight

through that flow. Along this 1-D domain, Navier–Stokes turbulence is not reproduced exactly but its effect is modeled by stochastically perturbing the velocity and scalar profiles. The conservation equations are therefore split into source terms, molecular diffusion, and stochastic re-arrangements (eddy events) along the 1-D domain, that is,

$$\frac{\partial u_i}{\partial t} + \mathscr{E}_i(u_j) = \nu \frac{\partial^2 u_i}{\partial y^2} + F_i, \tag{1}$$

$$\frac{\partial \theta}{\partial t} + \mathscr{E}_\theta(u_j) = \Gamma \frac{\partial^2 \theta}{\partial y^2} + S_\theta, \tag{2}$$

where y denotes the ODT line coordinate, t the time, u_i the velocity vector, θ the passive scalar, F_i the external forces, S_θ the scalar sources, ν the kinematic viscosity, Γ the scalar diffusivity, and $\mathscr{E}$ the eddy events. In equations (1) and (2) the eddy events depend only on the instantaneous velocity profiles $u_j(y,t)$. This is the ODT analog of the passive scalar, where only the velocity affects the selection and implementation of eddy events which we will discuss shortly. Note the subscripts θ and i to $\mathscr{E}$ which remind us of differences in the eddy implementation between the passive scalar and the velocity, respectively. $\mathscr{E}_i$ differs from $\mathscr{E}_\theta$ due to the inclusion of pressure-velocity correlations and the exchange of kinetic energy between the velocity vector components.

The eddy events are the fundamental building block of ODT. They are implemented by triplet-mapping the velocity and scalar profiles across an eddy of size l. This mimics the effect of turbulent stirring phenomenologically by steepening the property (scalar and velocity) gradients locally. The triplet map consists of (i) a compression of a property profile to a third of its original length, (ii) filling the interval by two copies of the compressed profile, and (iii) flipping the central copy to ensure continuity and conservation (for details see Kerstein, 1999).

The eddy size l and the position y_0 are sampled individually from approximate distributions since the actual eddy rate distribution $\lambda(l,y_0,t)$ is unknown. In ODT, $\lambda(l,y_0,t)\,\mathrm{d}l\,\mathrm{d}y_0$ gives the number of eddies in the size range $[l, l+\mathrm{d}l]$ and the position range $[y_0, y_0+\mathrm{d}y_0]$ during a time interval $[t, t+\mathrm{d}t]$. Dimensional analysis shows that $\lambda(l,y_0,t)$ is inversely proportional to the squared eddy size and the ODT analog eddy turnover time $\tau(l,y_0,t)$, that is,

$$\lambda(l,y_0,t) = \frac{C}{l^2\,\tau(l,y_0,t)}, \tag{3}$$

where C is the ODT turbulence intensity parameter. Since l/τ can be interpreted as a measure for the eddy velocity, a measure for the eddy specific kinetic energy is given by l^2/τ^2, which is related to the velocity field by (summation convention implied)

$$\frac{l^2}{\tau^2} \simeq u_{K,i}^2 + \alpha\, T_{ij}\, u_{K,j}^2 - Z\frac{\nu^2}{l^2}, \tag{4}$$

in which $u_{K,i}$ is the triplet-mapped and mapping-kernel-weighted velocity field, T_{ij} is the transfer tensor that models the kinetic energy exchange between the velocity components due to velocity-pressure correlations, α is the isotropy parameter, and Z is the viscous penalty parameter that effectively limits the smallest possible eddies. Equations (3) and (4) suggest that the extractable energy can be used to decide which of the candidate eddies are physical. That is, the larger the eddy energy l^2/τ^2, the larger the probability for eddy acceptance. A thinning-and-rejection algorithm ensures that the ODT results will not depend on the approximate distribution from which candidate eddies are sampled.

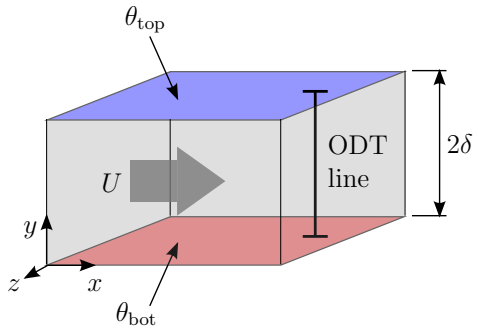

Figure 1. Sketch of the channel flow configuration investigated.

Note that the eddy energy and the eddy acceptance depend only on the instantaneous velocity field in the case of a passive scalar. Buoyant or reactive flows can be treated straightforwardly in ODT by an extension of the eddy energy formulation (for details see Lignell *et al.*, 2013). This leaves C, Z, and α as the core model parameters, which need to be optimized for the flow configuration under consideration.

The Channel Flow Configuration

Figure 1 shows a sketch of the channel flow configuration investigated in this study. We consider an incompressible, Newtonian fluid between the top and bottom wall. The flow is driven by a mean pressure gradient, which yields the force $F_x = -\rho^{-1}(\mathrm{d}P/\mathrm{d}x) = 1$ in equation (1). At the top and bottom wall, homogeneous no-slip conditions are used for the velocity ($u_{\mathrm{bot},i} = u_{\mathrm{top},i} = 0$) and Dirichlet boundary conditions prescribe the passive scalar ($\theta_{\mathrm{bot}} = +1$, $\theta_{\mathrm{top}} = -1$). There are no other sources sources for the passive scalar which yields $S_\theta \equiv 0$ in equation (2).

Here, the computational domain for the channel flow is simply the line segment denoted "ODT line" in figure 1 which spans the entire channel height 2δ in wall-normal direction y. In this setting, the streamwise (x) and spanwise (z) directions are taken to infinity and we assume that the flow is statistically stationary.

Optimization of the ODT Parameters

Modeling the turbulent transport of the momentum and the passive scalar together yields requirements that need to be met by adjusting the three ODT parameters. For the simulations of this work, the optimal parameters read $C = 6$ (turbulence intensity), $Z = 300$ (viscous penalty), and $\alpha = 1/6$ (anisotropy). The optimization aimed to match the mean and the r.m.s. profiles of the streamwise velocity (u) and the passive scalar (θ) of ODT and reference DNS results for channel flows at $Re_\tau = 180$ and 2000 with $Sc = 1$. The $Re_\tau = 180$ case was used to find combinations of ODT parameters that yield mean scalar and velocity profiles close to the reference DNS of Schwertfirm & Manhart (2007) and Moser *et al.* (1999) respectively. Then, the $Re_\tau = 2000$ case was used to confirm that the modified ODT parameters will reproduce the reference DNS velocity profile of (Lee & Moser, 2015).

The model parameters were kept fixed for the variation of the Schmidt and Reynolds number. We assured ourselves that simulations conducted for $Sc > 1$ do not exhibit significant changes in the velocity profile. It is due to the adaptive ODT solver implementation, however, that the velocity profiles exhibit a weak dependency on the Schmidt number due to a higher resolution of the velocity

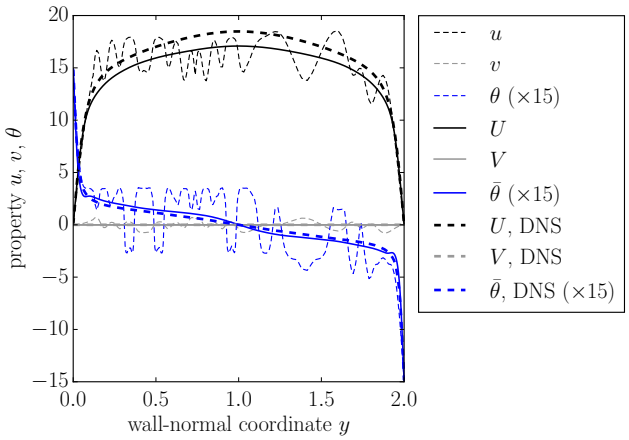

Figure 2. Simulated mean and instantaneous wall-normal profiles for a channel flow at $Re_\tau = 180$ and $Sc = 10$. DNS mean profiles from Moser *et al.* (1999, velocities) and Schwertfirm & Manhart (2007, passive scalar).

field with increasing Sc. This is a spurious effect at low Reynolds numbers and becomes negligible for $Re_\tau > 10^3$.

It is worth to mention that an optimization of the isotropy parameter α was essential for the present study. Usually, α is kept constant at $2/3$ to yield the fastest tendency towards small-scale isotropic turbulence (compare with Kerstein *et al.*, 2001). This is a bit different when ODT is used as stand-alone tool that also needs to resolve the non-universal large scales (see also Meiselbach, 2015).

Typical Scalar and Velocity Profiles

Figure 2 shows various simulated wall-normal profiles of the scalar (θ), the streamwise (u) and wall-normal (v) velocity components for $Re_\tau = 180$ and $Sc = 10$. Time-averaged profiles $\bar{\theta}(y)$, $U(y)$ and $V(y)$ obtained by ODT (thin solid lines) are shown in comparison to a corresponding DNS (thick dashed lines) of Schwertfirm & Manhart (2007) and Moser *et al.* (1999), respectively. Both $U(y)$ and $\bar{\theta}(y)$ exhibit steep gradients near the channel boundaries, which is a consequence of the Reynolds stresses that result from turbulent stirring. The passive scalar is affected even more by stirring since it exhibits a factor $Sc = 10$ slower diffusion time scale than the momentum. The wall-normal velocity vanishes on average ($V = 0$),

An example of instantaneous ODT property profiles $u(y,t)$, $v(y,t)$, $\theta(y,t)$ is also shown in figure 2 (thin dashed lines). One can see the combined effect of eddy events (triplet-mapping) and molecular diffusion (smoothing), which results in qualitatively similar perturbations of the profiles for u and θ. Looking carefully at the profiles reveals somewhat more details on the small-scales in the scalar profile, for example, as seen in the neighborhood of the local minima at $y \approx 0.5$, 1.0, 1.5 and the local maximum at $y \approx 1.3$.

It is remarkable that the time-averaged property profiles obtained by stand-alone ODT (figure 2) exhibit good qualitative, but also quantitative agreement with the reference DNS results. ODT appears to reproduce the near-wall structure of the mean profiles fairly well (to be discussed in more detail below), but at least for the low-Re_τ case shown, ODT underestimates the bulk streamwise velocity and overestimates the absolute value of the passive scalar in the bulk of the fluid. Slightly different values of the passive scalar are approached from the walls toward the centerline ($y = 1$) due to which the gradient steepens again there. There is no such feature visible in the DNS results, which hints at a slightly incorrect turbulent scalar transport representation within the present setup of stand-alone ODT.

Note further that the mean scalar profile in figure 2 exhibits a near-wall oscillation. The latter is likely related to the triplet map as discussed by Lignell *et al.* (2013).

In the next section, the statistical quantities of the passive scalar are investigated in the boundary layer to quantify ODT's ability to model turbulent scalar transport.

STATISTICAL ANALYSIS FOR VARIOUS SCHMIDT AND REYNOLDS NUMBERS

The variation of the Schmidt and Reynolds number was started with an initial long-time simulation for $Sc = 1$ and $Re_\tau = 180$ using homogeneous initial conditions. This simulation was continued for about 10^6 frictional time units ($t_\tau = \nu/u_\tau^2$) to gather statistics on the 1-D computational domain and to obtain property profiles in the statistically stationary state. The latter were used to initialize simulations at slightly larger values of Sc or Re_τ. The transient stage before gathering statistics was thus reduced to one third of the total simulation time.

The statistics were gathered over the last two thirds of the simulated time and an ensemble of $N = 4$ independent flow realizations. This yields a total of at least 4×10^5 frictional time units as statistical basis, which corresponds to an implementation of at least 10^5 ODT eddy events on the 1-D domain. We made sure that the last two sampling periods yield the same mean profile. So, basically, only the higher order statistics profit from a doubling of the sampling time interval. Note in this respect that the simulation time was shorter for larger Reynolds numbers, since an increase of the latter corresponds to an increase in the turbulence intensity or, likewise, an increase of the ODT eddy rate. For $Sc > 10^3$, the efficiency of ODT is notably reduced due to the resolution requirements imposed by the scalar, so that the simulation times were kept as low as possible. The high-Sc simulation results thus exhibit the smallest statistical ensembles.

In the following, all variables are expressed in friction units which is indicated by the superscript '+'. We use

$$y^+ = \frac{u_\tau}{\nu} y, \qquad \bar{\theta}^+ = \frac{\bar{\theta} - \theta_{\text{wall}}}{\theta_\tau},$$
$$\text{with} \qquad u_\tau = \sqrt{\nu \left| \frac{\mathrm{d}U}{\mathrm{d}y} \right|_{\text{wall}}}, \qquad \theta_\tau = \frac{\Gamma}{u_\tau} \left| \frac{\mathrm{d}\bar{\theta}}{\mathrm{d}y} \right|_{\text{wall}}. \quad (5)$$

First Order Statistics

Figure 3 shows various wall-normal profiles of the mean scalar concentration $\bar{\theta}^+(y^+)$ in semi-logarithmic scale for different Schmidt and Reynolds numbers. DNS results of Schwertfirm & Manhart (2007), DNS/LES results of Hasegawa & Kasagi (2009), and the conductive sublayer scaling ($\bar{\theta}^+ = Sc\, y^+$) are plotted for comparison. Good qualitative and quantitative agreement is observed between ODT and DNS/LES for all values of Sc and Re_τ investigated.

Quantitative agreement between ODT and DNS/LES is exhibited by the conductive sublayer for which the mean scalar gradient increases linearly with the Schmidt number, $(\mathrm{d}\bar{\theta}^+/\mathrm{d}y^+)|_{\text{wall}} = Sc$. The conductive sublayer scaling is met for $y^+ < 2\, Sc^{-0.29}$ (on the origin of the exponent 0.29 see Schwertfirm & Manhart, 2007).

Qualitative agreement between ODT and DNS/LES is exhibited across the logarithmic layer ($y^+ > 20\, Sc^{-0.29}$) by means that $\bar{\theta}^+$ increases nonlinearly with the Schmidt number. Stand-alone ODT, however, systematically underestimates $\bar{\theta}^+$ there. This effect is present also for low-Sc, but is only visible for $Sc \geq 49$ in the present scaling due to the large range of $\bar{\theta}^+$ values.

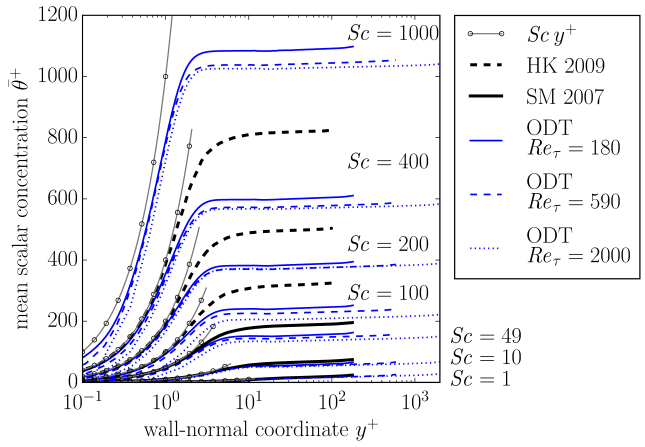

Figure 3. Semi-logarithmic plot of the wall-normal mean scalar profile for various Sc and Re_τ. Reference results are from Schwertfirm & Manhart (2007, $Re_\tau = 180$, DNS) and Hasegawa & Kasagi (2009, $Re_\tau = 150$, DNS/LES).

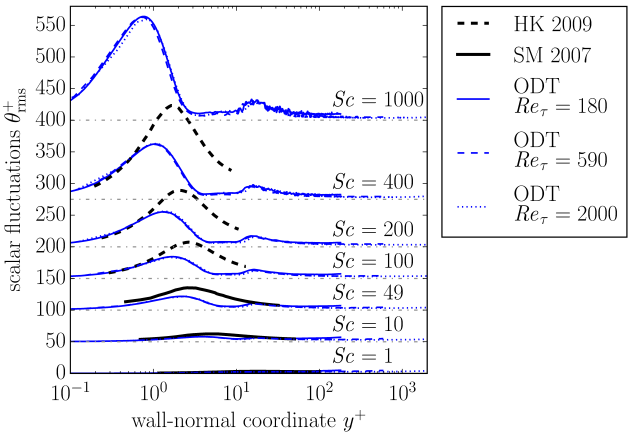

Figure 4. Semi-logarithmic plot of the wall-normal root mean square (r.m.s.) scalar fluctuation profiles for various Re_τ and Sc. The profiles are offset with increasing Sc to aid visualization and each corresponding base line ($\theta^+_{\mathrm{rms}} = 0$) is given by a dash-dotted horizontal line for orientation. Reference results are from Schwertfirm & Manhart (2007, $Re_\tau = 180$, DNS) and Hasegawa & Kasagi (2009, $Re_\tau = 150$, DNS/LES).

Table 1. Fitted coefficients κ_θ and B_θ parameterizing the logarithmic layer profile according to equation (6). Reference results are from Schwertfirm & Manhart (2007, $Sc \leq 49$, $Re_\tau = 180$, DNS) and Hasegawa & Kasagi (2009, $Sc \geq 100$, $Re_\tau = 150$, DNS/LES). The fits have been performed in the range $y^+ \in [40,\ 100]$ for turbulent flows at $Re_\tau = 180$ and 150, respectively.

Sc	$\kappa_\theta^{\mathrm{ODT}}$	B_θ^{ODT}	$\kappa_\theta^{\mathrm{DNS}}$	B_θ^{DNS}	$B_\theta^{\mathrm{ODT}}/B_\theta^{\mathrm{DNS}}$
1	0.25	-0.5	0.27	2.3	—
10	0.25	41.7	0.26	52.8	0.79
49	0.24	138.0	0.27	174.0	0.79
100	0.24	227.0	0.19	300.0	0.76
200	0.23	369.0	0.22	481.0	0.77
400	0.23	585.0	0.24	803.0	0.73
1000	0.21	1070.0	—	—	—

Interestingly, the logarithmic layer exhibits also quantitative agreement between ODT and DNS/LES but only with respect to the "slope" of the log law. This is not easily seen in figure 3, wherefore we fitted the simulated profiles with

$$\bar{\theta}^+(y^+) = \frac{1}{\kappa_\theta} \ln y^+ + B_\theta, \tag{6}$$

in which κ_θ is the von Kármán constant for the passive scalar and B_θ is a constant offset. Both κ_θ and B_θ may depend in general on Sc and Re_τ, but the ODT results in figure 3 suggest only a weak Re_τ-dependency. It needs to be clarified elsewhere if this is physically correct since the DNS/LES data available are not yet sufficient.

Table 1 shows the coefficients obtained by fitting equation (6) for $y^+ \in [40,\ 100]$ to various simulated mean scalar concentration profiles using a least-squares algorithm. Since $1/\kappa_\theta$ varies less with Sc than B_θ does, the ratio $B_\theta^{\mathrm{ODT}}/B_\theta^{\mathrm{DNS}}$ can be used approximately to quantify the ODT-bias of the mean scalar concentration throughout the logarithmic layer. As can be seen in table 1, this ratio is almost constant at around $B_\theta^{\mathrm{ODT}}/B_\theta^{\mathrm{DNS}} \approx 3/4$.

Note that the DNS of Schwertfirm & Manhart (2007) yield the von Kármán constant to be $\kappa_\theta^{\mathrm{DNS}} \approx 0.27$ for $Re_\tau = 180$ and $Sc \in [1,\ 49]$, but DNS/LES results of Hasegawa & Kasagi (2009) yield a $\approx 25\%$ lower value for a similar Reynolds number but $Sc \in [100,\ 400]$ (see table 1). It is interesting that stand-alone ODT is able to predict the value of κ_θ within this scatter of the DNS/LES results. We attribute the differences between stand-alone ODT and DNS/LES to originate primarily from the buffer layer, where ODT does not resolve 3-D flow features that seem to be crucial for the scalar transport. This suggests that the assumption of featureless turbulence, which underlies ODT, is acceptable for the logarithmic layer, but not for the buffer layer. As a consequence, the turbulent scalar transport seems to be inhibited across the buffer layer in stand-alone ODT, which might explain the lower $\bar{\theta}^+$-value observed throughout the logarithmic layer (figure 3).

We assess the hypothesis of less turbulent transport across the buffer layer in ODT with the aid of the fluctuation statistics in the following section.

Second Order Statistics

Figure 4 shows wall-normal profiles of the root mean square (r.m.s.) scalar fluctuations $\theta^+_{\mathrm{rms}}(y^+)$ in semi-logarithmic scale for different Schmidt and Reynolds numbers. DNS results of Schwertfirm & Manhart (2007) and DNS/LES results of Hasegawa & Kasagi (2009) are plotted for comparison in a reduced range of values. To aid visibility, the profiles for different Schmidt numbers are plotted with a vertical offset in steps of $\Delta\theta^+_{\mathrm{rms}} = 50$ for $Sc \leq 200$, $\Delta\theta^+_{\mathrm{rms}} = 75$ for $Sc = 400$, and $\Delta\theta^+_{\mathrm{rms}} = 125$ for $Sc = 1000$. The shifted zero-lines are dash-dotted for these cases. Small fluctuations for $Sc = 1000$ indicate that that the statistical ensemble should be enlarged if a smoother profile is required.

The r.m.s. profiles shown in figure 4 exhibit good qualitative but also quantitative agreement between stand-alone ODT and DNS/LES. Quantitative agreement is observed in the vicinity of

the wall ($y^+ < 5\,Sc^{-0.29}$) and in the logarithmic layer ($y^+ > 20$). There, the magnitude of the scalar fluctuations is reproduced correctly, which seems to agree well with the result of the previous section: ODT performs well near the wall and throughout the logarithmic layer. However, only qualitative agreement is observed in the buffer layer discussed in the following.

In the DNS/LES results shown in figure 4, the onset of a near-wall peak can be discerned at around $y^+_{\max} \approx 5$ for $Sc = 10$. The onset of this peak is captured by stand-alone ODT for precisely the same Sc and approximately at the same location, but the r.m.s.-peak seems a bit weaker in magnitude than in the reference DNS/LES. With increasing Sc, this peak increases in magnitude and moves closer to the wall. The reference DNS/LES exhibit the maximum at $y^+_{\max} \approx 4$ for $Sc = 49$ and at $y^+_{\max} \approx 1.5$ for $Sc = 400$. The corresponding peak in the ODT results, however, appears much closer to the wall, is smaller in magnitude, and is accompanied by a local minimum at some further distance from the wall ($3 < y^+_{\min} < 10$ in dependence on Sc). This local minimum is not present in the DNS/LES solution. However, this deficiency in the fluctuations (and presumably in the turbulent scalar transport) affects only the mean scalar concentration as discussed above, whereas the scalar r.m.s. values themselves agree rather well with the reference DNS/LES throughout the logarithmic layer. Altogether, the r.m.s. values support the assertion of less turbulent scalar transport across the buffer layer within ODT.

It is worth to note that the spatial oscillation in the ODT scalar r.m.s. profiles (figure 4) corresponds to the spurious near-wall oscillation noted earlier for the mean scalar concentration (figure 2). A similar spatial structure has been observed by Lignell *et al.* (2013) for the velocity r.m.s. values. These authors suggest that the reason is to be seen in the near-wall eddy events, which turn out self-similar due to the form of the triplet map and almost identical in value due to the conservation properties of ODT. Hence, subsequent near-wall eddy events possess a large overlap so that temporal averaging cannot remove the triplet-map structure from the statistical quantities. Here, with respect to the scalar fluctuations (figure 4), the side effect is that ODT cannot develop the near-wall peak since the spurious spatial oscillation interferes with or even replaces the r.m.s. peak expected from the DNS/LES.

Interestingly, the scalar fluctuation profiles obtained by stand-alone ODT shown in figure 4 collapse almost exactly for the different Reynolds numbers investigated. This suggests that the turbulent transport of a passive scalar is merely independent of the Reynolds number, which is surprising given the range of Re_τ investigated. It is also not quite expected, since it contradicts the weak Re_τ-dependency observed for the mean scalar profiles (figure 3). Again, further research is needed to clarify the Re_τ-dependency of the turbulent scalar transport.

SCALAR MASS TRANSFER COEFFICIENT

The results discussed in the previous section have shown that ODT is able to reproduce the mean and fluctuation statistics of the reference DNS/LES throughout the conductive sublayer very well, which is a prerequisite for computation of the scalar mass transfer across the wall. In the following, the scalar mass transfer coefficient obtained by stand-alone ODT is compared to available DNS/LES results and laboratory measurements.

The scalar mass transfer coefficient K^+ "parameterizes" the scalar mass flux across the wall by an easy-to-measure scalar concentration difference. This coefficient is defined as

$$K^+ = \frac{\theta_\tau}{\Delta\theta}, \tag{7}$$

which is the reciprocal scalar concentration difference between the bulk (channel centerline) and the wall, $\Delta\theta = \bar{\theta}_{\text{bulk}} - \theta_{\text{wall}}$, measured in units of the friction scale θ_τ (see equation (5)). For channel flows, $\bar{\theta}_{\text{bulk}}$ is the mean scalar concentration at the centerline ($y = \delta$ as in Schwertfirm & Manhart, 2007).

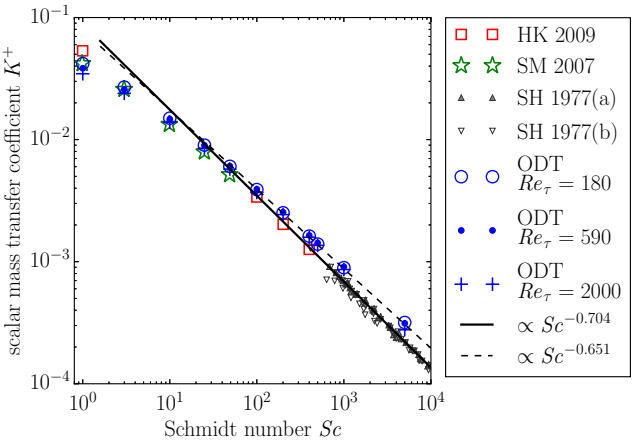

Figure 5. Double-logarithmic plot of the scalar mass transfer coefficient K^+ as function of the Schmidt number Sc for various Reynolds numbers Re_τ. Reference results are from Schwertfirm & Manhart (2007, $Re_\tau = 180$, DNS) and Hasegawa & Kasagi (2009, $Re_\tau = 150$, DNS/LES), two types of reference laboratory measurements at high Re_τ are from Shaw & Hanratty (1977, labeled a, b).

Figure 5 shows the scalar mass transfer coefficient $K^+(Sc)$ as function of the Schmidt number obtained for various Reynolds numbers in a double-logarithmic plot. ODT results for low-to-high Re_τ are shown in comparison to low-Re_τ DNS/LES results (Schwertfirm & Manhart, 2007; Hasegawa & Kasagi, 2009), as well as measurements in a high-Re_τ regime obtained from two different configurations (Shaw & Hanratty, 1977). Good qualitative and quantitative agreement is observed between ODT, DNS/LES, and laboratory measurements by means that K^+ values of similar magnitude are obtained for corresponding Sc and Re_τ, and by means that K^+ becomes independent of the Reynolds number for high Schmidt numbers, here $Sc > 10^2$.

Moreover, the results in figure 5 show that measured and simulated K^+ exhibit the power law

$$K^+ \propto Sc^a \qquad \text{for} \qquad Sc \to \infty. \tag{8}$$

Laboratory measurements yield $a_{\text{lab}} = -0.704$, whereas, theoretically, a scaling exponent of $a_{\text{theo}} = -2/3$ or $-3/4$ is expected depending on the structure of the boundary layer (Shaw & Hanratty, 1977). The "intermediate" value of the measured exponent hints at a more complicated behavior in reality than is covered by existing theory.

In order to elucidate the scaling exponent, numerical results have been conducted and reported a relatively large spread of values ($-0.7 < a < -0.5$, e.g. Na *et al.*, 1999; Schwertfirm & Manhart, 2007; Hasegawa & Kasagi, 2009). Interestingly, only the reference DNS/LES results of Hasegawa & Kasagi (2009) for $Sc \geq 100$ in figure 5 exhibit the scaling exponent of the laboratory measurements. The power-law scaling according to equation (8) breaks down for Schmidt numbers smaller than 100 due to a Re_τ-dependency of the scalar transport (see Schwertfirm & Manhart, 2007).

It is worth to point out that the K^+ values obtained by stand-alone ODT (figure 5) collapse on the same values for Schmidt

numbers $Sc > 10^2$ for all Reynolds numbers investigated. The ODT results exhibit a clear power-law scaling over a broad range of Schmidt numbers and exhibit the scaling exponent $a_{\mathrm{ODT}} \approx -0.651 \pm 0.011$, which has been obtained by a least-squares fit of equation (8) to the K^+ values obtained for $Re_\tau = 180$, 590, and 2000 in the range $Sc \in [10^2,\ 10^4]$.

Furthermore, it is interesting that ODT results of K^+ agree well with the DNS/LES results also at low and moderate Schmidt numbers (see figure 5 for $Sc < 10^2$). At $Sc = 1$, ODT and the reference DNS of Schwertfirm & Manhart (2007, $Re_\tau = 180$, channel) yield almost the same value of K^+ for corresponding Re_τ, but there is a notable difference to the DNS/LES of Hasegawa & Kasagi (2009, $Re_\tau = 150$, wall). In the latter a slightly different configuration and a lower Reynolds number flow was used. This case is dominated by non-universal, system-scale flow features, but since the momentum and passive scalar transport are strongly coupled by exhibiting the same advective and diffusive time scales, it seems to be a low-Reynolds-number effect that leads to a difference in the mass transfer coefficients at $Sc = 1$ between ODT and the reference DNS.

Altogether, by the aid of ODT we have been able to simulate high-*Sc* turbulent scalar transport in flow regime which is presently inaccessible by DNS. Given the simplicity of ODT, it is amazing that simulated values of K^+ are less than a factor two (2) larger than the measured values. No modification of the ODT parameters took place, which indicates that ODT is a robust tool for turbulent transport modeling up to very high Schmidt numbers.

SUMMARY AND CONCLUSION

We studied the turbulent transport of a passive scalar up to very high Schmidt numbers (up to $Sc = 5000$) in fully-developed, turbulent channel flows at various Reynolds numbers (up to $Re_\tau = 2000$) using the stochastic One-Dimensional Turbulence (ODT) model as stand-alone tool. ODT results were compared to available reference data from DNS, LES, and laboratory measurements with respect to profiles of the mean scalar concentration and the mean streamwise velocity, the root mean square (r.m.s.) scalar fluctuations, and the scalar mass transfer coefficient. In general, good qualitative and quantitative agreement has been obtained, but some differences between the ODT and the reference results are notable.

On the upside, ODT is able to capture most of the relevant flow features. In the logarithmic layer, ODT yields a von Kármán constant for the passive scalar of $\kappa_\theta^{\mathrm{ODT}} = 0.23 \pm 0.02$. This value is very close to the reference DNS/LES, which yield $\kappa_\theta^{\mathrm{DNS}} = 0.23 \pm 0.04$. This suggests that ODT is able to model the turbulent scalar transport accurately in the logarithmic layer.

In particular, note that the mean scalar concentration (figure 3) and the r.m.s. values (figure 4) obtained by ODT are in very good agreement with the reference DNS/LES throughout the conductive sublayer. Consequently, the scalar mass transfer coefficient K^+ (figure 5) exhibits agreement between ODT and the reference DNS/LES. The ODT results for K^+ exhibit the power law $K^+ \propto Sc^a$ with the exponent $a_{\mathrm{ODT}} = -0.651 \pm 0.011$ for Schmidt numbers $Sc > 100$. This is very close to the reference value $a_{\mathrm{lab}} = -0.704$ obtained by laboratory measurements. This suggests that the near-wall scalar transport and the near-wall scalar concentration are both fairly accurately modeled by ODT.

On the downside, the scaled mean scalar concentration (figure 3) is systematically underestimated in ODT throughout the logarithmic layer by a factor of $\approx 3/4$ in comparison to the reference DNS/LES. In addition, the r.m.s. values (figure 4) obtained by ODT are significantly lower than in the reference DNS/LES in the buffer layer, say $1 < y^+ < 10$, where the logarithmic and the conductive layer overlap. Both of the latter deficiencies hint at an inaccurate representation of the buffer layer dynamics within stand-alone ODT. This means that ODT is neither able to resolve nor to mimic crucial 3-D flow features (as shown, e.g., by Hasegawa & Kasagi, 2009).

In conclusion, we suggest that ODT exhibits less advective transport across the buffer layer, which results in a lower mean scalar concentration throughout the logarithmic layer. Due to continuity constraints on the scalar profile, diffusion is enhanced within ODT to maintain a constant scalar mass flux across the channel.

It is worth to emphasize the numerical efficiency of ODT in the light of the few deficiencies mentioned. The sum of the simulations presented here took a total of ≈ 8500 CPU-h on a few local workstations. This renders ODT an ideal tool for studying turbulent transport in a wide range of control parameter values, here exemplified by *Sc* encompassing about four orders of magnitude.

At last, we note that the limitations of stand-alone ODT with respect to 3-D flow structure representation can be resolved by using ODT as efficient and accurate sub-grid scale model in an LES framework: so-called ODTLES (e.g. Glawe *et al.*, 2013; Glawe, 2015). Such an undertaking, however, is beyond the scope of this study, but it seems worth to assess high-*Sc* turbulent scalar transport with ODTLES in the future.

REFERENCES

Batchelor, G. K. 1959 Small-scale variation of convected quantities like temperature in turbulent fluid. Part 1. General discussion and the case of small conductivity. *J. Fluid Mech.* **5**, 113–133.

Glawe, C. 2015 ODTLES: Turbulence modeling using a one-dimensional turbulence closed extended large eddy simulation approach. PhD thesis, Freie Universität Berlin, Berlin, Germany.

Glawe, C., Schulz, F. T., Gonzalez-Juez, E. D., Schmidt, H. & Kerstein, A. R. 2013 ODTLES simulations of turbulent flows through heated channels and ducts. *Proc. 8th Int. Symp. Turb. Shear Flow Phen. (TSFP8)* **2**, 1–6, session 4C/3, URL: www.tsfp-conference.org/proceedings/2013/v2/htc.pdf.

Hasegawa, Y. & Kasagi, N. 2009 Low-pass filtering effects of viscous sublayer on high Schmidt number mass transfer close to a solid wall. *Int. J. Heat and Fluid Flow* **30**, 525–533.

Kerstein, A. R. 1999 One-dimensional turbulence: model formulation and application to homogeneous turbulence, shear flows, and buoyant stratified flows. *J. Fluid Mech.* **392**, 277–334.

Kerstein, A. R., Ashurst, W. T., Wunsch, S. & Nilsen, V. 2001 One-dimensional turbulence: vector formulation and application to free shear flows. *J. Fluid Mech.* **447**, 85–109.

Lee, M. & Moser, R. D. 2015 Direct numerical simulation of turbulent channel flow up to $Re_\tau \approx 5200$. *J. Fluid Mech.* **774**, 395–415.

Lignell, D. O., Kerstein, A. R., Sun, G. & Monson, E. I. 2013 Mesh adaption for efficient multiscale implementation of one-dimensional turbulence. *Theor. Comp. Fluid Dyn.* **27**, 273–295.

Meiselbach, F. T. 2015 Application of ODT to turbulent flow problems. PhD thesis, Brandenburgische Technische Universität Cottbus - Senftenberg, Cottbus, Germany.

Moser, R. D., Kim, J. & Mansour, N. N. 1999 Direct numerical simulation of turbulent channel flow up to $Re_\tau \approx 590$. *Phys. Fluids* **11** (4), 943–945.

Na, Y., Papavassiliou, D. V. & Hanratty, T. J. 1999 Use of direct numerical simulation to study the effect of Prandtl number on temperature fields. *Int. J. Heat and Fluid Flow* **20**, 187–195.

Ostilla-Monico, R., Yang, Y., van der Poel, E. P., Lohse, D. & Verzicco, R. 2015 A multiple-resolution strategy for direct numerical simulation of scalar turbulence. *J. Comp. Phys.* **301**, 308–321.

Schwertfirm, F. & Manhart, M. 2007 DNS of passive scalar transport in turbulent channel flow at high Schmidt numbers. *Int. J. Heat and Fluid Flow* **28**, 1204–1214.

Shaw, D. A. & Hanratty, T. J. 1977 Turbulent mass transfer rates to a wall for large Schmidt numbers. *AIChE Journal* **23** (1), 28–37.